

Fresh State Requirements for 3D Printable Mortar Mix

Isabelle Gerges^{1,4}, Faten Abi Farraj², Nicolas Youssef³, Fadi Hage Chehade¹, Emmanuel Antczak⁴

¹Lebanese University, Beirut Lebanon & Artois University, Arras, France
isabelle.gerges@ul.edu.lb ; fchehade@ul.edu.lb

² Advanced Construction Technology Services (ACTS), Beirut, Lebanon
fabifarraj@acts-int.com

³ ICL, Junia, Université Catholique de Lille, LITL, F-59000 Lille, France
nicolas.youssef@junia.com

⁴Univ. Artois, IMT Nord Europe, Junia, Univ. Lille, ULR 4515, Laboratoire de Génie Civil et géoEnvironnement (LGCgE), F-62400 Béthune, France
emmanuel.antczak@univ-artois.fr

Abstract - Significant innovations have been achieved in the building sector with the use of 3D printing technology, which enables the printing of complex structures with less time, labor, waste, and costs. The key quest in this technology is to have a printable material that must achieve several requirements in order to be printable, such as achieving good flowability and then structural stability after extrusion, otherwise, this can cause damage to the printer and potentially lead to greater maintenance expenses. Therefore, this research uses laboratory tests to check the fresh state properties that the mix must achieve in order to be printable. Slump, slump flow, manual device gun, slug test, uniaxial unconfined compression test, and vicat apparatus have been used to characterize the formulated mix at fresh state and check its printability. These tests are simple to use, require less manual labor, materials, time to prepare, and provide fast results with little post-processing needs. A good prediction of the material behaviour has been obtained using these tests, checking that the material achieves the general fresh state properties flowability, extrudability, buildability, and open time. Then, checking the elevation of yield stress and green strength in function of time in order to ensure that the material can be buildable and sustain its weight without any failure. Finally, these tests have given a good sign for having an appropriate printability by successfully printing multiple shapes without any failure.

Keywords: 3D printing - Mortar mix - General Fresh state properties - Laboratory tests - Rheological properties – Mechanical fresh state properties - Printability

1. Introduction

Applications of 3D printing technology in the construction sector are numerous and are supposed to increase in the future surpassing the planet Earth to reach the Moon and Mars [1]-[2]-[3]. 3D printable concrete combines the benefits of self-compacting concrete with no need for vibration and formworks enabling the creation of free-form construction with sophisticated designs [4]-[5]-[6]. However, Due to the layer-by-layer construction process, the properties of 3D printing material differ from conventional construction [7]. 3D printable material should satisfy general fresh state properties to have a flowable material in the pumping system, extrudable material through the nozzle with a continuous filament without any disruption, and buildable material that can sustain its weight and upper layers without any failure due to the lack of formwork [8]. These properties have to be verified in a longer time to maintain good printability, which is known as open time [9]. Researchers have assessed these properties by several laboratory tests such as the slump, slump flow, rheometer, penetration test, plate stacking test, etc.

For quantifying the mix, rheological and mechanical fresh state properties are also assessed by researchers. The rheological properties that are widely verified are the static yield stress which is the amount of stress required to start a flow, and the thixotropy in terms of structural buildup which refers to the increase of yield stress with time [10]. Different stages of material behavior should the 3D printed mortar succeed in having a printable material. Before extruding material, the static yield stress of the material should be low to have good flowability [11]. After deposition, the elevation of yield stress is essential to have shape retention and the material can sustain its weight. To sustain the upper layer, an increase in yield stress over time is required for proper printing [7]. Rheometers are used to assess the rheological properties. If they are

unavailable, researchers have utilized equations to correlate and link the yield stress and structural buildup with several tests such as the slump, shear vane, and slug tests [12]-[13].

Since rheological properties specifically static yield stress cannot be measured at an advanced time after extrusion, or the rheometer cannot measure high value of yield stresses, mechanical fresh state properties are also assessed. When the printing of material takes a long time or if a huge or complicated structure has to be printed, mechanical fresh state properties in terms of green strength and stiffness have to be proven with an increasing rate to not have plastic or buckling collapse [14]-[15]. Uniaxial unconfined compression test and penetration test are used to characterize the mechanical fresh state properties [16].

In this research, fresh state characterization of a mix was assessed using laboratory tests, followed by checking the printability. A total of six tests were evaluated to check the fresh state properties. These tests are slump, slump flow, manual device gun, slug test, unconfined compressive test, and vicat apparatus. First, the slump flow and manual device gun were used to check the general fresh state properties flowability, extrudability, buildability, and open time. Then, the characterization gets deeply by quantifying the mix and obtaining the rheological properties in terms of static yield stress and structural build-up using the slump, slump flow, and slug test by doing correlation using equations used previously by researchers. Then, the mechanical properties at fresh state were assessed using the unconfined compressive test and the vicat apparatus to check the evolution of green strength with time and the setting time of the mortar. Finally, after conducting all these steps and obtaining their properties, the mix was checked by the printer to check its printability

2. Material and Mix Design

The mortar constituents used in this research are, Portland-Limestone cement Type I-L which contains less clinker content than ordinary Portland cement (6 to 15%) limestone content, leading to less CO₂ emissions. Silica fume was used as supplementary cementitious material to reduce the cement content and lower the CO₂ emissions. As for the aggregates, fine crushed limestone sand with a maximum aggregate size of 2 mm was obtained from a Lebanese quarry by crushing limestone rocks. To reduce the water/binder ratio and still have good workability, a higher range water reducer hyperplasticizer "EPSILONE HP 565" from Weber Saint-Gobain was used.

The mortar mix design composition is presented in Table 1. The binder contains 90% Portland limestone cement and 10% silica fume. The aggregate-to-binder ratio was set to 2.4 and the water-to-binder to 0.3. The dosage of admixture was set to 1% relative to the cement weight.

The process utilized for the mixing procedure consists of mixing first at low speed the cement, sand, and silica fume for 4 min. Then, water and superplasticizer were added, and mixed for 3 minutes at a low speed and then 3 minutes at a medium speed.

Table 1: Mortar mix compositions with respect to binder weight.

Cement/binder	Silica fume/binder	Sand/binder	Water/binder	Superplasticizer ^a
0.9	0.1	2.4	0.3	1%

^a (% of cement weight)

2. Tests Used

The tests used to characterize the mix at fresh state illustrated in Fig. 1 are slump, slump flow, manual gun, slug test, unconfined compression test, and vicat apparatus.

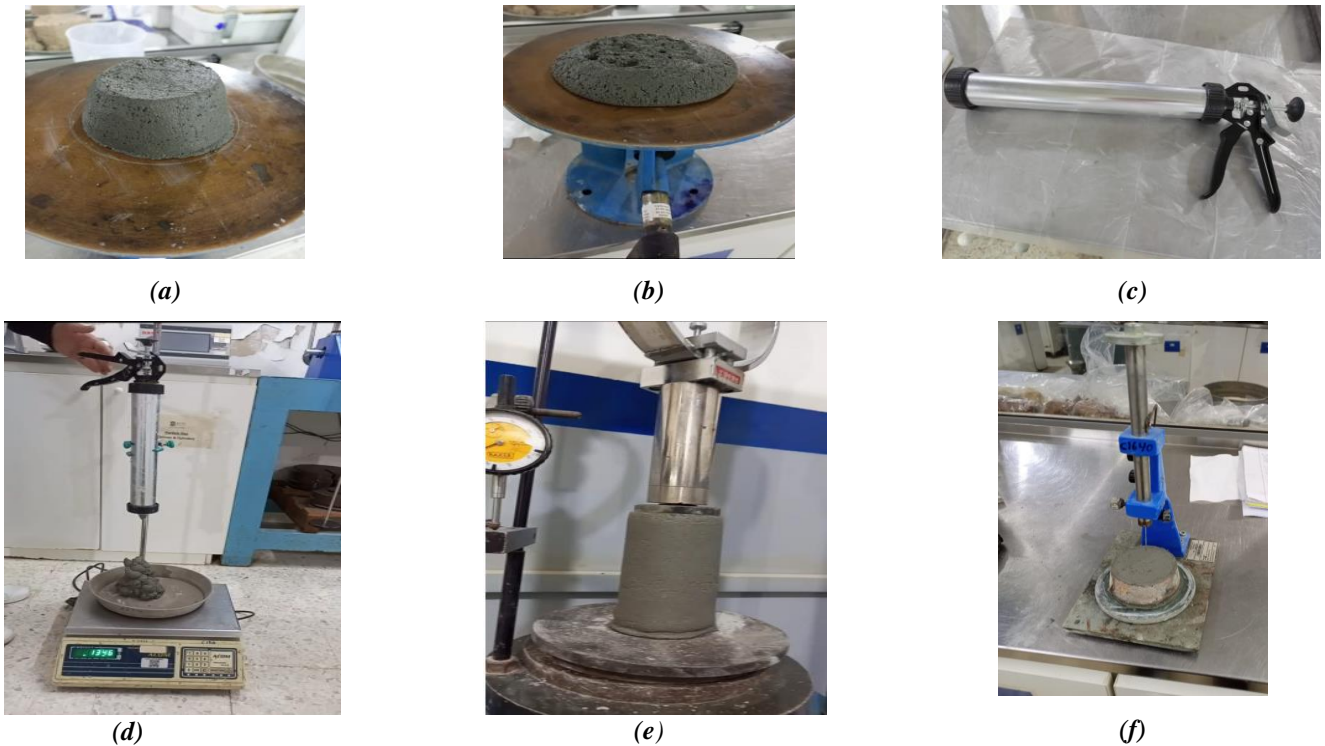


Fig. 1: Tests used for fresh state characterization of the mortar mix (a) Slump (b) Slump flow (c) Manual device gun (d) Slug test (e) uniaxial unconfined compression test (f) Vicat apparatus.

Slump and slump flow tests were done in accordance with ASTM C230. The slump test consists of tamping 20 times 2 layers, then the mold is removed and the difference height is recorded as the slump value. The protocol for the slump flow continues in conformance with ASTM C1437 after removing the mold by dropping the flow table 25 times and recording the slump flow diameter.

A manual device gun with a hose diameter of 19.4 mm was used by filling it with mortar and checking if the mix was extrudable by having a continuous filament. Then, stacking layer upon layer to check if the material satisfies the buildability properties without any failure.

The slug test used recently by various researchers [13]-[15]-[17], was used for the characterization process in this research. This test that measures the yield stress was carried out using a manual device gun that was held vertically and filled with fresh mortar. Then, the extruded mortar stretched until its weight exceeded the cohesive forces, where mortar dropped in the form of separate slug masses creating discrete slug masses. 20 droplets were collected and weighed on a balance to determine the weight of the slug masses.

Unconfined uniaxial compression test (UUCT) that is used widely in the 3D printing research domain [18]-[19]-[20] for the quantification of the fresh properties of the mortar mix by measuring the green strength, was used in this study. The test is adapted from the traditional UUCT standard for soil specimens, ASTM D2166. The cylindrical UUCT samples used have an aspect ratio of 2, with a height of 150 mm and a diameter of 75 mm. They were prepared in three layers, and each layer was compacted 25 times with a tamping rod. The samples were then placed in the testing system and an unconfined uniaxial compression test was performed using a tabletop compression machine in a displacement-controlled mode at a rate of 10 mm/min. The compressive green strength was obtained by dividing the peak force by the surface area of the mortar specimen.

To measure the initial and final setting time of concrete, the vicat apparatus was assessed. The vicat can evaluate the hydration and flocculation rate of materials, which further determines the stiffness development of 3DPC. The test procedure

was done as ASTM C191. The initial setting time was recorded when the needle penetrates 25 mm and the final setting time was recorded when the penetration didn't leave any mark on the surface of the specimen.

First, a rapid and visual inspection of the slump flow and the manual device gun will be used to check the general fresh state properties flowability, extrudability, buildability, and open time. The slump, slump flow, and slug tests will then be used to determine the rheological properties and the evolution of the yield stress with time. Then, the uniaxial unconfined compression test and the Vicat apparatus will be used to check the mechanical fresh state properties.

3. Results Obtained

3.1. General Fresh State Properties Assessment

Simple tests might be performed and visually inspected to start characterizing the mix and determine whether the material satisfies all of the general fresh state properties, including flowability, extrudability, buildability, and open time. Therefore, the slump flow test and the manual device gun have been used to check these properties.

In previous studies, researchers have proven the printability of their mixes using the slump flow test and the manual device gun. They concluded that the slump flow diameter must be in defined ranges like 150-190 mm [21], 186-210 mm [22], otherwise, the material couldn't be printable. Using the manual device gun, they concluded that extruding filaments and stacking them on top of each other without any failure provide an appropriate sign of extrudability, buildability, and open time properties [23]-[24].

Therefore, these tests were performed to confirm the suggested mix, and a comparison was made to evaluate what would happen if the w/b increased to 0.35 or decreased to 0.28.

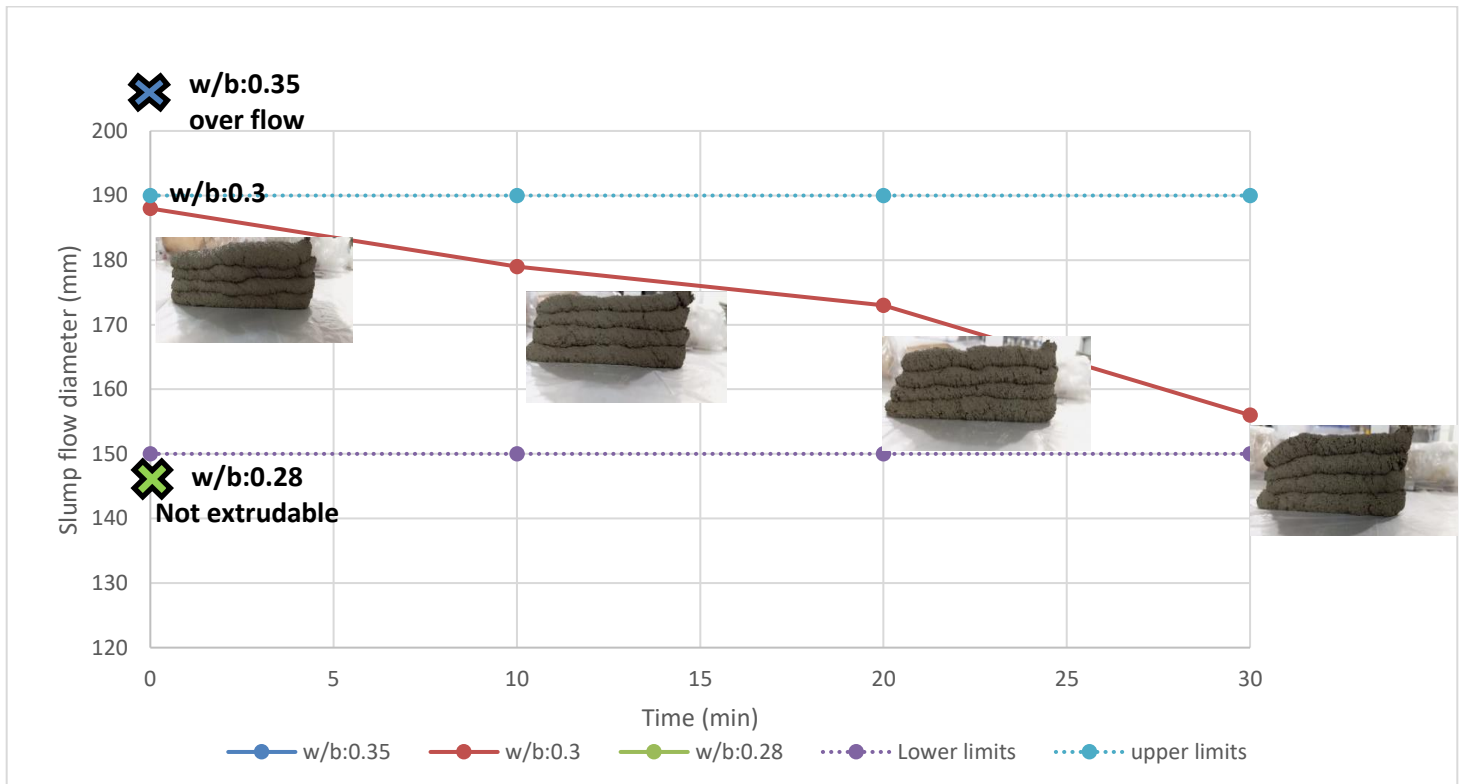


Fig. 2: Printable zone checking by slump flow test and manual device gun.

The slump flow diameter value presented in Fig. 3 indicates that the diameter reduced from 188 to 156 mm within 30 minutes. In addition, using the manual device gun, the mix was extrudable with a continuous filament of 150 mm length

without any disruption and buildable by stacking four layers on top of each other without showing any failure. Mortar was checked in 30 minutes intervals, and the material was extrudable and buildable at all times, resulting in a good open time. To check the printability zone and make sure to choose the right mix proportion, the water-to-binder ratio was increased to 0.35 and decreased to 0.28. For a w/b ratio of 0.35 the material was very flowable and we couldn't get a value from the slump flow because the material fell from the flow table after 25 drops. Furthermore, for 0.28 w/b, the slump flow value after the mixing was 146mm. Nevertheless, the material was not extrudable when tested for extrudability using the manual device gun. Therefore, the mix with 0.35 and 0.28 w/b were eliminated because they didn't meet any of the general fresh state properties.

Using this general characterization, we could define the margin printability for slump flow value that should be between 190 and 150 mm because higher than these values the material will be flowable and lower than these values the material will be stiff. Furthermore, the extrudability and buildability by visual inspection using the manual gun and checking if the material can be extruded without any problem and buildable and can sustain layers without failure.

3.2. Rheological Properties Assessment

Since there is a link between the general fresh state properties and the rheological properties, the rheology of the mix was assessed. In 3D printing for the material to be flowable and then printable, the material yield stress should be low for optimal fluidity. After extrusion, high yield stress is required to allow the bottom layer to support the upper layer. Therefore, the structural buildup which corresponds to " A_{thix} " is an important parameter that corresponds to the increase of yield stress with time after the layer's deposition so the material can sustain its upper layer. Roussel [25] describe that the yield stress increases linearly in the function of time and the relation is presented as follows:

$$\tau_{c(t)} = \tau_{0,0} + A_{thix}t \quad (1)$$

where A_{thix} is the structuration rate, $\tau_{0,0}$ is the initial yield stress, and $\tau_{c(t)}$ is the yield stress after deposition with respect to time.

To determine the rheological properties and when the rheometer test is unavailable, several tests could be used to study and correlate the properties, especially the static yield stress [26].

The tests that will be used in this research for quantifying the rheological properties are slump, slump flow, and slug test. Roussel and Coussot [27] correlate the slump test to the yield stress by:

$$\tau_c = \frac{\rho g (H - z_c)}{\sqrt{3}} \quad (2)$$

where H is the height of the sample and z_c is the critical height when the flow stops.

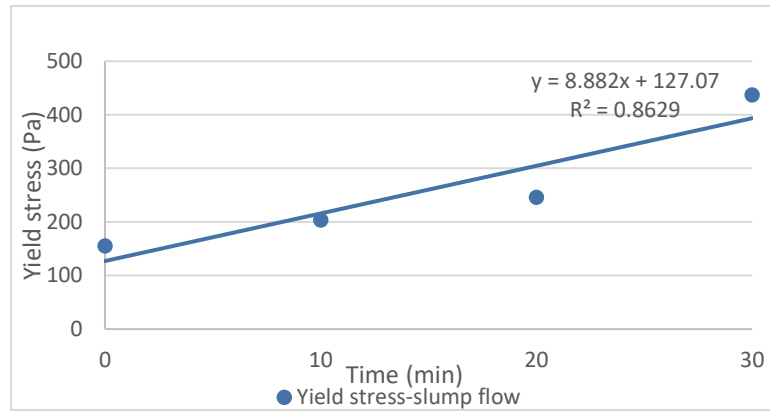
Regarding the slump flow, The approach that will be used to obtain the yield stress is according to Shin and Kim[28], where D is the slump flow diameter value:

$$D = 466 \tau_c^{-0.18} \quad (3)$$

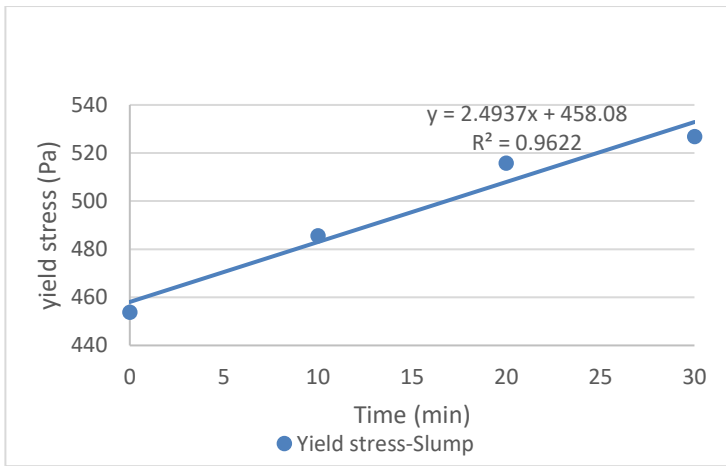
Regarding the slug test, the slug masses were used to measure the yield stress of concrete according to Equation (4) given by Ducoulombier et al.[13], where τ_c , g , S , m_s represent the slug test yield stress, average mass of slugs, gravitational acceleration, nozzle sectional area, and average mass of slugs calculated by dividing the total collected mass " m_t " by " n " the number of slugs:

$$\tau_c = \frac{g}{\sqrt{3} S} m_s \quad (4)$$

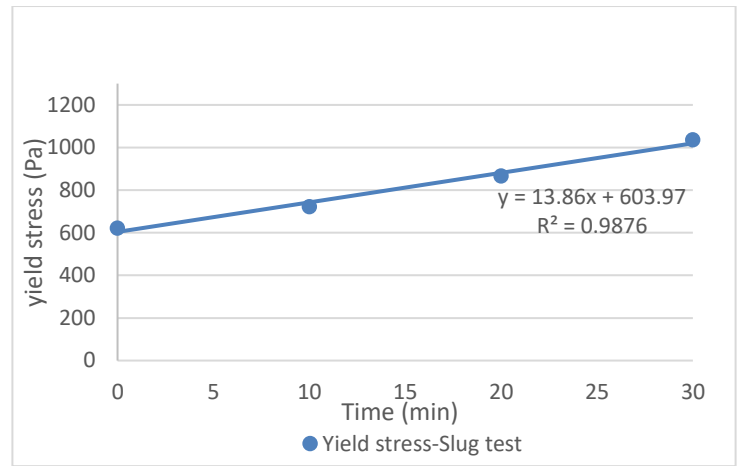
Using these formulas, the yield stress was calculated over 30 minutes. After that period, the yield stress cannot be calculated due to the inability to execute the slug test. Fig. 4 represents the graphs that show the evolution of yield stress in function of time, depicting the structural buildup A_{thix} .



(a)



(b)



(c)

Fig. 4: Structural buildup determined by means of (a) Yield stress using slump flow (b) Yield stress using slump (c) Yield stress using slug test.

Linear increase in the yield stress using all the tests used was seen in Fig. 4 as Roussel [25] depict in equation (3). In these equations "x" represents the concrete age, "y" describes the yield stress after deposition in time, whereas the coefficient of x presents the rate of structural build-up, as measured by the conventional test methods.

All the 3 graphs show a good linear fitting curve having a coefficient of determination R^2 higher than 0.85. The structuration rate adopted from the slump flow and slug test was close by having a value of 8.882 Pa/min and 13.86 Pa/min. Nevertheless, the structural buildup obtained from the slump test was lower in order of 2.4937 Pa/min compared to the other tests due to the low slump values that were 16, 14.5, 12.5, and 12mm for 0,10,20, and 30 min. The minimum slump value leads to low development of structural buildup, and this was demonstrated by various studies [15]-[16].

3.3. Mechanical Properties at Fresh State Assessment

In 3D printing, rapid growth in strength is required to provide good printability and no failure during or after printing. Therefore, the layers especially the lower layer must exhibit a rapid increase in green strength to achieve vertical stability and prevent plastic collapse. For this reason, the evolution of early-age mechanical strength was examined since it deserves more attention while printing the desired structure.

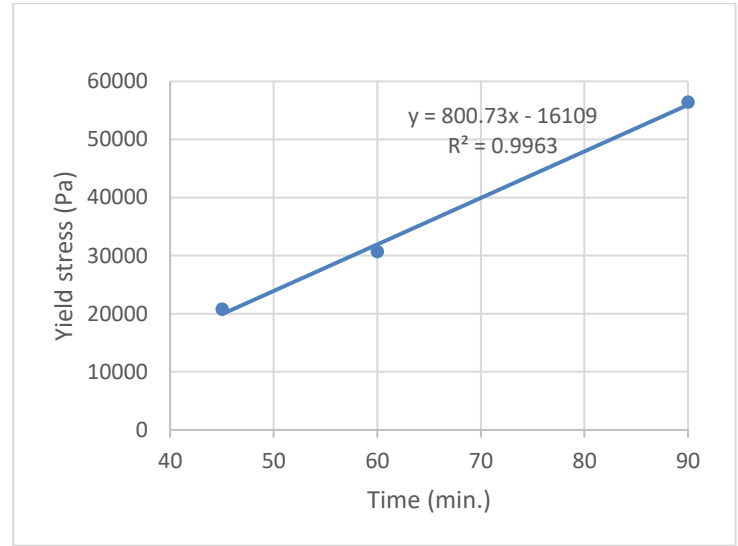
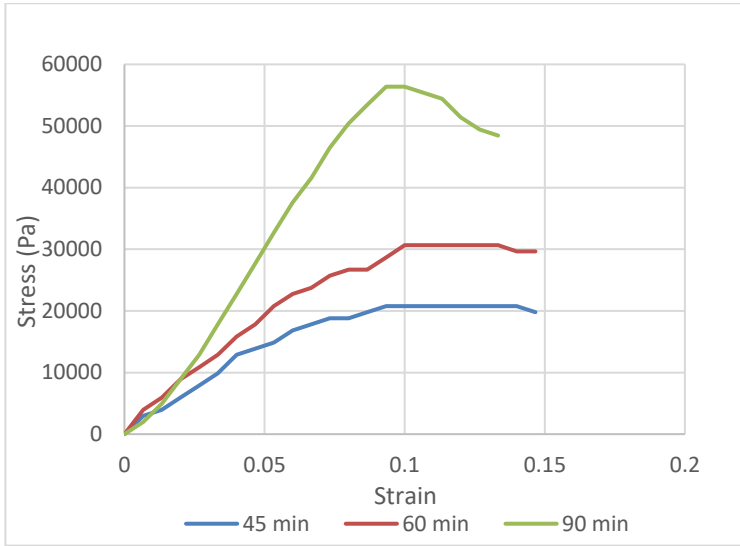


Fig. 5: Results obtained from UUCT (a) Evolution of stress-strain curve in the function of time (b) Evolution of green strength in the function of time.

The tests that will be used in this research to measure the mechanical fresh state properties are the uniaxial unconfined compression test UUCT which measures the compressive strength of the fresh mortar at a given time and the vicat apparatus which is the simplest test method that evaluates the hydration rate of the mix by giving the initial and final setting time.

Using the UUCT test,

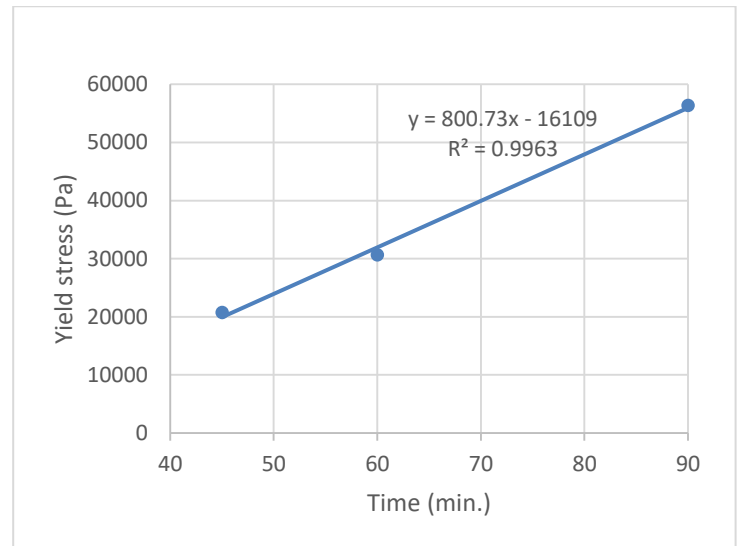
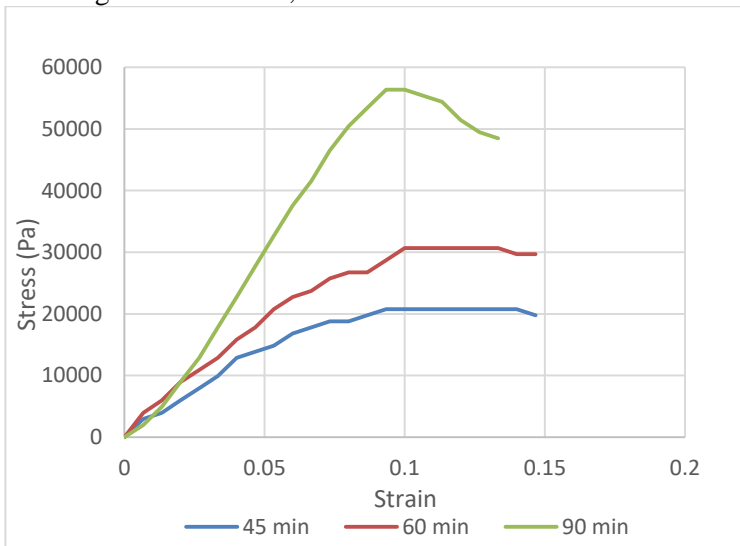


Fig. 5(a) depicts the change in the pattern of compressive stress versus strain curves at three different ages 45, 60, and 90 min of mortar. The compressive stress increases first linearly with the strain. However, the linear region for 45 and 60 min is shorter than 90 min due to the continuous hydration of the cement and the higher internal structural buildup with increasing time. Then, after attaining the peak, the compressive stress decreases with higher strain. It should be noted that the critical strain at 90 min shifts to the left, while the compressive stress increases. As shown in

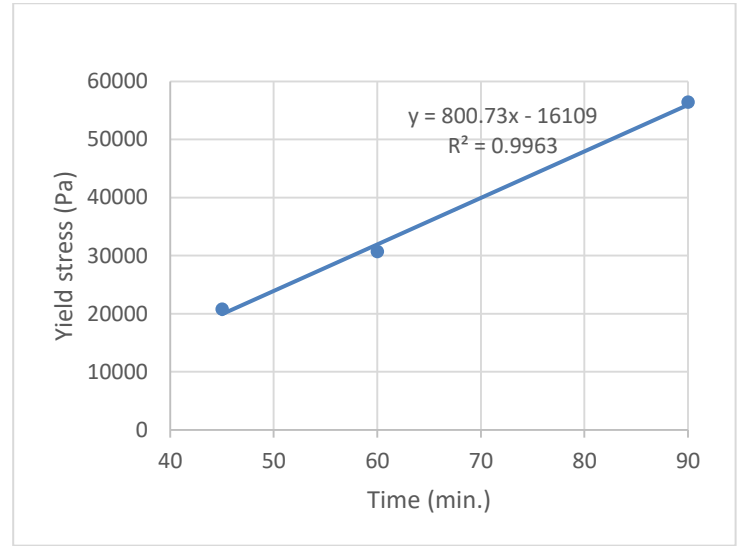
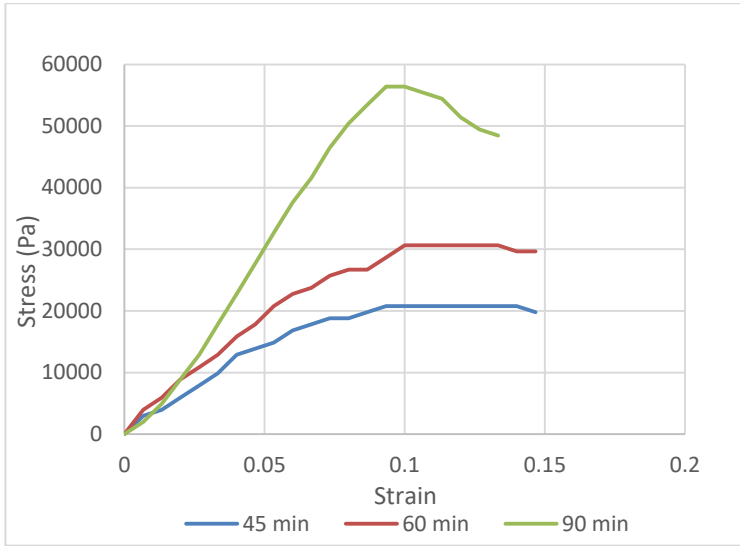


Fig. 5(b), The peak of the stress-strain curve that was taken as the compressive strength value was plotted in function of time. The graph shows a good linear fitting curve. The green strength develops from 20772 Pa to 56381 Pa from 45 min to 90 min with a structuration rate of 800.73 Pa/min. The higher green strength and structuration rate compared to the yield stress was obtained due to the mortar's higher structural buildup in advanced hours which is essential in 3D printing to not have any plastic collapse if we have a long or complicated printing structure.

Vicat apparatus was performed to check the setting behavior of mortar which refers to how the fluidity and stiffness change from casting to final hardening. The initial setting time that we obtained was 105 min and the final setting time was 165 min. In 3D printing, various studies found that a high setting time of about 160 min exhibited minimum buildability. Therefore, the initial setting time for 3D printing should be low and within these ranges 110, 147, and 120 min [23]-[29]-[30], in order to produce a printable material that gains strength faster than conventional concrete and can support its weight and upper layer without any deformation and this is what we have obtained in this characterization.

3.4. Printability Checking

After the deep fresh state characterization, the mix was checked by the printer. The printer is a gantry type, as seen in Fig. 6, with a circular nozzle of 16 mm and a bed size and height of 530x530x1000 mm in x, y, and z directions.

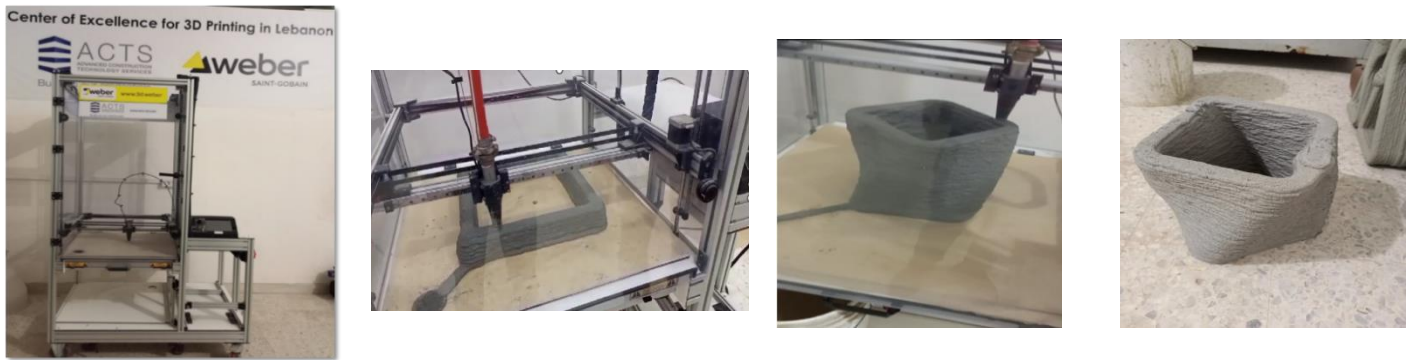


Fig. 6: Printed objects by a gantry printer using the characterized mix

As illustrated in Fig. 6, the mix has been printed without any failure. Various shapes have been printed using the characterized mix. A rectangular shape was printed with 12 layers and a layer thickness of 8mm and a width of 50 ± 5 mm. In addition, an articulated column shape was printed without any failure with 41 layers, a thickness of 6 mm, and a width of 30 ± 5 mm.

4. Conclusion

This study aimed to check the fresh state requirements using laboratory tests to have a 3D printable mortar mix. Various tests have been used in this study to characterize the mix at fresh state like slump, slump flow, manual device gun, slug test, uniaxial unconfined compression test, and vicat apparatus.

It was concluded by using rapid and visual inspection that the slump flow diameter must be between 150 and 190 mm to succeed the general fresh state properties flowability, extrudability, buildability, and open time. Below 150 mm, the material will be very stiff and will not get out from the manual device gun, while above 190 mm, the material will be very flowable.

To quantify the mix and check the rise in static yield stress and green strength over time, the rheological and mechanical fresh state properties were assessed. The rheological examination using slump, slump flow, and slug tests shows the linear evolution of static yield stress with time, which starts low for optimal flowability and then increases gradually for shape retention and stability. The mechanical fresh state properties were then examined using the UUCT and Vicat apparatus. The UUCT test showed a significant increase in green strength and a high structuration rate value, which is essential for a stable structure without any deformation or failure over time. This improvement in strength was also demonstrated by having a low setting time using the Vicat device.

The assessment and characterization of the mortar mix using these tests has given a good sign for having a printable material by printing rectangular shape with up to 12 layers and articulated shape with up to 41 layers while exhibiting strong stability and no failure during or after printing.

Acknowledgements

This research is financially supported by Advanced Construction Technology Services (ACTS). The authors express their sincere gratitude to all of its employees for their financial and technical assistance.

References

- [1] B. Khoshnevis, "Automated construction by contour crafting—related robotics and information technologies," *Autom. Constr.*, vol. 13, no. 1, pp. 5–19, Jan. 2004, doi: 10.1016/j.autcon.2003.08.012.
- [2] J. Morgan, "Work on world's first 3D-printed skyscraper to begin in Dubai by 2023 - Construction Week Online." Accessed: Jul. 04, 2024. [Online]. Available: <https://www.constructionweekonline.com/projects-tenders/article-46835-work-on-worlds-first-3d-printed-skyscraper-to-begin-in-dubai-by-2023>
- [3] AI Spacefactory, "LINA," AI Spacefactory. Accessed: Jul. 04, 2024. [Online]. Available: <https://spacefactory.ai/lina>
- [4] B. Nematollahi, M. Xia, and J. Sanjayan, "Current Progress of 3D Concrete Printing Technologies," presented at the 34th International Symposium on Automation and Robotics in Construction, Taipei, Taiwan, Jul. 2017. doi: 10.22260/ISARC2017/0035.
- [5] A. Saleh Abd Elfatah, "3D Printing in Architecture, Engineering and Construction (Concrete 3D printing)," *Eng. Res. J.*, vol. 162, no. 0, pp. 119–137, Jun. 2019, doi: 10.21608/erj.2019.139808.
- [6] R. Jemghili, A. Ait Taleb, and K. Mansouri, "Additive Manufacturing Progress as a New Industrial Revolution," in *2020 IEEE 2nd International Conference on Electronics, Control, Optimization and Computer Science (ICECOCS)*, Kenitra, Morocco: IEEE, Dec. 2020, pp. 1–8. doi: 10.1109/ICECOCS50124.2020.9314623.
- [7] A. U. Rehman and J.-H. Kim, "3D Concrete Printing: A Systematic Review of Rheology, Mix Designs, Mechanical, Microstructural, and Durability Characteristics," *Materials*, vol. 14, no. 14, p. 3800, Jul. 2021, doi: 10.3390/ma14143800.

- [8] T. T. Le, S. A. Austin, S. Lim, R. A. Buswell, A. G. F. Gibb, and T. Thorpe, “Mix design and fresh properties for high-performance printing concrete,” *Mater. Struct.*, vol. 45, no. 8, pp. 1221–1232, Aug. 2012, doi: 10.1617/s11527-012-9828-z.
- [9] Z. Li, M. Hojati, Z. Wu, J. Piasente, N. Ashrafi, J.P. Duarte, S. Nazarian, S.G. Bilén, A.M. Memari, A. Radlińska, “Fresh and Hardened Properties of Extrusion-Based 3D-Printed Cementitious Materials: A Review,” *Sustainability*, vol. 12, no. 14, p. 5628, Jul. 2020, doi: 10.3390/su12145628.
- [10] A. Perrot, D. Rangeard, and A. Pierre, “Structural built-up of cement-based materials used for 3D-printing extrusion techniques,” *Mater. Struct.*, vol. 49, no. 4, pp. 1213–1220, Apr. 2016, doi: 10.1617/s11527-015-0571-0.
- [11] D. Marchon, S. Kawashima, H. Bessaies-Bey, S. Mantellato, and S. Ng, “Hydration and rheology control of concrete for digital fabrication: Potential admixtures and cement chemistry,” *Cem. Concr. Res.*, vol. 112, pp. 96–110, Oct. 2018, doi: 10.1016/j.cemconres.2018.05.014.
- [12] N. Q. Dzuy and D. V. Boger, “Yield Stress Measurement for Concentrated Suspensions,” *J. Rheol.*, vol. 27, no. 4, pp. 321–349, Aug. 1983, doi: 10.1122/1.549709.
- [13] N. Ducoulombier, R. Mesnil, P. Carneau, L. Demont, H. Bessaies-Bey, J.-F. Caron, N. Roussel, “The ‘Slugs-test’ for extrusion-based additive manufacturing: Protocol, analysis and practical limits,” *Cem. Concr. Compos.*, vol. 121, p. 104074, Aug. 2021, doi: 10.1016/j.cemconcomp.2021.104074.
- [14] N. Roussel, “Rheological requirements for printable concretes,” *Cem. Concr. Res.*, vol. 112, pp. 76–85, Oct. 2018, doi: 10.1016/j.cemconres.2018.04.005.
- [15] A. U. Rehman, A. Perrot, B. M. Birru, and J.-H. Kim, “Recommendations for quality control in industrial 3D concrete printing construction with mono-component concrete: A critical evaluation of ten test methods and the introduction of the performance index,” *Dev. Built Environ.*, vol. 16, p. 100232, Dec. 2023, doi: 10.1016/j.dibe.2023.100232.
- [16] A. U. Rehman, I.-G. Kim, and J.-H. Kim, “Towards full automation in 3D concrete printing construction: Development of an automated and inline sensor-printer integrated instrument for in-situ assessment of structural build-up and quality of concrete,” *Dev. Built Environ.*, vol. 17, p. 100344, Mar. 2024, doi: 10.1016/j.dibe.2024.100344.
- [17] Y. Jacquet, A. Perrot, and V. Picandet, “Assessment of asymmetrical rheological behavior of cementitious material for 3D printing application,” *Cem. Concr. Res.*, vol. 140, p. 106305, Feb. 2021, doi: 10.1016/j.cemconres.2020.106305.
- [18] A. L. Van Overmeir, S. C. Figueiredo, B. Šavija, F. P. Bos, and E. Schlangen, “Design and analyses of printable strain hardening cementitious composites with optimized particle size distribution,” *Constr. Build. Mater.*, vol. 324, p. 126411, Mar. 2022, doi: 10.1016/j.conbuildmat.2022.126411.
- [19] A. L. Van Overmeir, B. Šavija, F. P. Bos, and E. Schlangen, “3D printable strain hardening cementitious composites (3DP-SHCC), tailoring fresh and hardened state properties,” *Constr. Build. Mater.*, vol. 403, p. 132924, Nov. 2023, doi: 10.1016/j.conbuildmat.2023.132924.
- [20] I. Ivanova, E. Ivaniuk, S. Bisetti, V. N. Nerella, and V. Mechtcherine, “Comparison between methods for indirect assessment of buildability in fresh 3D printed mortar and concrete,” *Cem. Concr. Res.*, vol. 156, p. 106764, Jun. 2022, doi: 10.1016/j.cemconres.2022.106764.
- [21] Y. W. D. Tay, Y. Qian, and M. J. Tan, “Printability region for 3D concrete printing using slump and slump flow test,” *Compos. Part B Eng.*, vol. 174, p. 106968, Oct. 2019, doi: 10.1016/j.compositesb.2019.106968.
- [22] J. Teixeira, C. O. Schaefer, L. Maia, B. Rangel, R. Neto, and J. L. Alves, “Influence of Supplementary Cementitious Materials on Fresh Properties of 3D Printable Materials,” *Sustainability*, vol. 14, no. 7, p. 3970, Mar. 2022, doi: 10.3390/su14073970.
- [23] N. Khalil, G. Aouad, K. El Cheikh, and S. Rémond, “Use of calcium sulfoaluminate cements for setting control of 3D-printing mortars,” *Constr. Build. Mater.*, vol. 157, pp. 382–391, Dec. 2017, doi: 10.1016/j.conbuildmat.2017.09.109.
- [24] G. Ma, Z. Li, and L. Wang, “Printable properties of cementitious material containing copper tailings for extrusion based 3D printing,” *Constr. Build. Mater.*, vol. 162, pp. 613–627, Feb. 2018, doi: 10.1016/j.conbuildmat.2017.12.051.
- [25] N. Roussel, “A thixotropy model for fresh fluid concretes: Theory, validation and applications,” *Cem. Concr. Res.*, vol. 36, no. 10, pp. 1797–1806, Oct. 2006, doi: 10.1016/j.cemconres.2006.05.025.

- [26] N. Roussel, C. Stefani, and R. Leroy, “From mini-cone test to Abrams cone test: measurement of cement-based materials yield stress using slump tests,” *Cem. Concr. Res.*, vol. 35, no. 5, pp. 817–822, May 2005, doi: 10.1016/j.cemconres.2004.07.032.
- [27] N. Roussel and P. Coussot, “‘Fifty-cent rheometer’ for yield stress measurements: From slump to spreading flow,” *J. Rheol.*, vol. 49, no. 3, pp. 705–718, May 2005, doi: 10.1122/1.1879041.
- [28] T. Y. Shin and J. H. Kim, “First step in modeling the flow table test to characterize the rheology of normally vibrated concrete,” *Cem. Concr. Res.*, vol. 152, p. 106678, Feb. 2022, doi: 10.1016/j.cemconres.2021.106678.
- [29] Chen, Li, Chaves Figueiredo, Çopuroğlu, Veer, and Schlangen, “Limestone and Calcined Clay-Based Sustainable Cementitious Materials for 3D Concrete Printing: A Fundamental Study of Extrudability and Early-Age Strength Development,” *Appl. Sci.*, vol. 9, no. 9, p. 1809, Apr. 2019, doi: 10.3390/app9091809.
- [30] J. G. Da Silveira Júnior, K. De Moura Cerqueira, R.C. De Araújo Moura, P.R. De Matos, E.D. Rodriguez, J.R. De Castro Pessôa, M. Tramontin Souza, “Influence of Time Gap on the Buildability of Cement Mixtures Designed for 3D Printing,” *Buildings*, vol. 14, no. 4, p. 1070, Apr. 2024, doi: 10.3390/buildings14041070.